Version of Record: https://www.sciencedirect.com/science/article/pii/S0141933119300493
Manuscript_9e68d741cdeb328bf1e9ad3255e3d046

OFDM-based Electrical Impedance Spectroscopy Technique for Pacemaker-Induced Fibrosis Detection Implemented in an ARM Microprocessor

[1,3]Edwin De Roux, [1]Mehdi Terosiet, [1]Florian Kölbl, [2]Michel Boissière, [1]Aymeric Histace and [1]Olivier Romain

[1]Laboratoire ETIS, Université Paris Seine, Université de Cergy-Pontoise, ENSEA, UMR8051
[2]Laboratoire ERRMECe, EA1391, Université de Cergy-Pontoise, France
[3]SENACYT and Universidad Tecnológica de Panamá, Rep. de Panamá

ARTICLE INFO

keywords:
Electrical impedance spectroscopy
Broadband measurement
OFDM
ARM microprocessors

ABSTRACT

Fibrosis represents an open issue for medium to long-term active implants, such as pacemakers, given that this biological medium surrounds the stimulation electrodes and can impact or modify the performances of the system. For this reason, Embedded Impedance Spectroscopy (EIS) techniques have been investigated these last years to sense the fibrosis. The following article introduces a new technique for EIS derived from multi-carrier digital communication methods. Due to its properties of flat spectrum and fast generation the Orthogonal-Frequency Division Multiplexing (OFDM) technique for EIS represents an efficient and a low foot-print alternative compared to the classical sweep frequency technique. This article focuses on this approach and also proposes a solution that reduces the effect of high crest factor typically found in OFDM systems. An embedded implementation is also presented. This designed prototype is used here to characterize the impedance spectrum of a pacemaker's electrode achieving an accuracy of 99% when measuring with 64 OFDM subcarriers and with a sampling frequency of 12 kHz.

1. Introduction

Technological advances in micro-nano-electronics permit the development of implantable devices that help in the treatment of health disorders. Implants like pacemakers, cochlear prosthesis, cardiac defibrillators, deep-brain neuro-stimulators, insulin pumps, etc. are generally placed under the skin or implanted deeply in the body. However, this intervention produces an immune response that involves inflammation and the growth of a dense tissue encapsulation, known as fibrosis, which affects the electrical capabilities of the device. Fibrosis could be medically or electrically compensated only after being sensed [1].

With some medical treatments the fibrosis can be reduced, but its effectiveness depends on the accurate diagnosis. Histology represents the standard method for determining the degree of tissue reaction surrounding the electrodes, but this method is not in situ and requires an invasive extraction of tissue material. The immunohistochemical technique enables the visualization of specific markers like collagen, fibronectin or smooth muscle actin [2]. Most of them are inappropriate to follow the tissue reaction in real time in vivo [3].

Alternative methods, like optical ones, have been investigated. The most efficient of this kind is based on the conjunction of Late Gadolinium Enhancement and Cardiac Magnetic Resonance (CMR) techniques. This procedure is used to detect fibrosis in cardiac tissues, even if it is scattered and in low concentration [4]. However, its effectiveness decreases when the patient carries a pacemaker. This latter has the particularity to sparkle and to cause some artifacts on the image. In addition, due to risk factors, it is contraindicated to apply CMR in patients with PCM, and even if this is done, it is recommended to carry it out weeks after post-implant surgery, which allows a considerable accumulation of fibrous tissue on the electrodes [5].

Chronic monitoring of tissue alteration around implanted electrodes could be a first step to understand this long-term biological process. This advance could be used to ascertain the treatment effectiveness or to test new biocompatibility strategies of materials. For instance, electrical impedance spectroscopy (EIS) has proven to be a useful technique in the continuous monitoring of biological tissues that, together with electrical modeling, enables the detection and parameterization of biological activities [6].

A typical EIS system consists in an electronic device, that generates stimulations over different frequencies and that senses the electrical signal, coming from the Sample Under Test (SUT), usually by using a metallic electrode that has a physical contact with the SUT. The most common implementation, even in commercial instruments, is the frequency sweep technique. Here the stimulation signal is a sine wave whose frequency is modified in each impedance calculation.

There are several challenges for the implantable integration of rapid measurement of fibrosis by EIS. The frequency sweep technique requires an extensive exploratory time, especially at low frequencies [7]. For the detection of pacemaker-induced fibrosis, the measurement time should be shorter than the time between cardiac pulsations. Therefore, a faster method is

needed. Multi-frequency signals such as multi-sine have been investigated, for instance in [8] and [9], to accelerate the measurement, but they suffer from a large foot-print memory that limits the integration.

In this article we propose a new method for EIS measurement that can be implemented in a low cost device, but still maintaining a good performance in the calculation of the impedance. It is based on the OFDM technique, well-known in digital communications [10], that simplify the design of the stimulation signal by choosing the appropriate OFDM symbol's properties. Furthermore, since the main drawback of the OFDM method is the probability of high crest factor (CF) of the modulated signal [11], we also propose the use of squared related phases OFDM symbols as a solution. A high CF, which is the ratio between the maximum amplitude and the Root Mean Squared (RMS) of a signal, is not desirable because this implies the appearance of high amplitude peaks in the stimulation signal that could induce heart palpitations during the measurement.

Although OFDM was first developed in the 1960s, only in recent years, this method has become available and used for telecommunications due to the increased performance of reconfigurable hardware, like FPGAs, and programmable devices such as general purpose microprocessors and dedicated Digital Signal Processors (DSP).

DSP provides fast vector multiplication by SIMD instruction and hardware, and some flexibility in the design could be achieved. However, the development of efficient solutions requires a great effort in programming [12]. Besides, FPGAs combine the speed power and density advantage of ASICs and the flexibility and reprogram ability of general purpose processors. Therefore, FPGAs are a better option for OFDM systems in telecommunications applications, where high speed processing is required at both low cost and low foot-print [13]. However, while the FPGA represents the best candidate to implement an efficient massive parallel architecture, its energy efficiency is reduced for floating point computations which could limit the implementation of our proposal.

Giving that our OFDM method has floating point computation in the last part of the impedance estimation, as it will be shown in Section 4, this proposed OFDM technique has been implemented here in sequential devices. Additionally, since low-power microprocessor architectures are available in the market, such as Cortex M0, these ones represent a good alternative for the design of an integrated version of the OFDM technique for a low cost and low power consumption OFDM-based Electrical Impedance Spectroscopy (OFDM-EIS) solution, with a minimum of development time.

The article is structured as follows: It begins with a state of art of EIS techniques and our new method for impedance measurements of pacemaker-induced fibrosis. The next section describes the implementation of the method in a general purpose microprocessor, follows the description of its functionalities and the method for calibration and impedance estimation. The OFDM-EIS method is then analyzed through experiments carried out with an accurate known impedance and with a real pacemaker electrode. In this section the crest factor is measured as well. At the end, this study is concluded with a brief synthesis and the presentation of the future works.

2. EIS overview

The EIS applied to the analysis of a biological material consists of injecting an alternating current or voltage into the tissue under study, and then measuring the resultant (voltage or current, respectively) that appears through the stimulation electrodes. There are several alternating signal generation methods for EIS used for this purpose, with their advantages and disadvantages. These will be discussed next.

2.1. Classic methods for EIS

The most common signal found in almost all commercial available EIS instruments, due to its implementation simplicity, is the fixed frequency sinusoidal signal. Here the measurements are carried out at a specific frequency, as in the case for these full-custom designs [*10, 11*], or in a small set of frequencies such as it is found in the commercial instrument xCELLigence [14] which measures the impedance at three discrete frequencies.

When the frequency sweep technique is used, the spectroscopy could be performed within a larger set of determined frequencies. The impedance analysis on a large frequency range provides more insights regarding the tissue features. Gabriel et al. measured the impedance of various organs of the human body in different conditions. The obtained frequency responses are specific signatures for each tissue [15]. This technique presents some limitations in the estimation of time-varying systems or when the impedance estimation of multiple electrodes or samples are needed in a short time frame by the same device. Due to these restrictions, this method does not meet the requirements of the proposed strategy.

2.2. Broadband EIS

Different methods for the generation of broadband signals have been investigated to overcome the limitation of classic approaches.

The first approach is dated back to 1975 where pseudo-random binary signals were used for the measurement of the impedance of an electrode in a wide frequency band [16]. The impedance impulse response is obtained by correlating the SUT signal output with the pseudo-random stimulus signal. In the case of Maximum Length Sequence (MSL) a more efficient method than correlation has been proposed in [17] based on the Fast Hadamard transform. This kind of signals contains a large range of frequencies and for this reason allows a fast impedance spectrum measurement. In addition, pseudo-random signals or MLS are preferred instead of the Dirac pulse, whose high amplitude peak is not desirable for the stimulation of biological samples [18, 19]. The main drawback of this method is the signal amplitude variation at each frequency. The spectrum of an MLS signal is also random and it is possible that the energy at a desired frequency

could be too low or equal in amplitude to the noise, which would induce errors in the measurement.

2.3. Multi-sine approach

Multi-sine approach for impedance spectrum measurement of biological samples, reported for instance in [20, 21] and [22], provides also a fast estimation with the advantage that the CF can be improved when using random phases and also that the frequencies can be selected as required, *i.e.* linear or logarithmic [23]. Such approach is simple, however does not scale easily with higher numbers of frequencies. The memory required for the generation of the multi-sine increases with the number of tones [24].

The stimulation part of a multi-sine system could be implemented in digital form by storing in memory the externally created multi-sine signal. However, the receiving part requires a more complex hardware for the demodulation of the signal, usually implemented by the use of a data acquisition board or system, such as an oscilloscope, and a Personal Computer (PC) for the impedance computation.

2.4. OFDM

Finally, OFDM combines a wide spectrum and a rapid impedance estimation in a large frequency bandwidth of interest, with the generation of a unique waveform. The generation of this kind of signals could be efficiently implemented by using the FFT algorithm [25]. This OFDM technique is successfully used in the field of digital communication, however its application to impedance measurement is a novelty and requires modifications, such as those presented in Section *3*.

The OFDM method controls the spectrum of the stimulation signal with great flexibility by defining the values of the OFDM symbols, the use of an appropriate modulation scheme and / or the manipulation of the system parameters, such as the sampling frequency.

The memory resources required to embed the OFDM-EIS method is analyzed by comparing it with previously described EIS techniques, for instance frequency sweep and multi-sine. Table 1 and Figure 1 show the amount of memory in words (16 bits in our application) for these approaches as a function of the quantity of measuring frequency *N/2*.

For the frequency sweep approach, there are *N*/2 different sinus to store in memory. Taking the same frequencies as the generated by the OFDM and if the sampling frequency is *Fs*, then the smaller frequency is *Fs*/*N*, the highest is *Fs*/2 and the frequency separation is also *Fs*/*N*. Therefore, for the creation of the tables containing one period of each sinus, it is needed: *N* samples for the frequency *Fs*/*N*, *N*/2 samples for the frequency 2*Fs*/*N*, and so on up to the frequency *Fs*/2 with only 2 samples in one period. However, in practice the sampling frequency is fixed at 10 times higher than the maximum frequency of the sweep requiring, in this case, even more memory.

The multi-sine approach is analyzed in two cases. The first one is the worst case scenario design where *N*/2 sinusoids are independently stored in memory and added for the creation of the multi-sine. For the reduction of the crest factor, it is advisable to apply different random phases to each sinus of the multi-sine signal. Considering that the multi-sine has the same quantity of samples that one symbol of the OFDM signal, which is *N*, then total required memory is $\frac{N}{2} \times N = \frac{N^2}{2}$.

The second case of the multi-sine involves storing the sum of the *N*/2 sinus, previously and externally calculated. Here the required memory is *N*. However, in this case the flexibility of modifying the spectrum of the stimulation signal is lost, requiring the recalculation of the multi-sine signal and the reprogramming of the system whenever, for instance, some frequencies are canceled or the frequency resolution is changed.

In the case of the proposed OFDM method, the length of the complete stimulation signal is $N \times M = N^2$. However, at the beginning of the cycle *N* samples are generated for the computation of the IFFT requiring only *N* memory words for the storage of the signal, given that the IFFT algorithm performs in-place calculation. Once they are sent, the OFDM system re-computes the new symbol of *N* samples and continues in this cycle until reaching *M* symbols. The IFFT algorithm has *N* sine/cosine coefficients (W^{kn}) in a normal mode and $\frac{N}{4}+1$ coefficients if optimized (avoiding coefficient redundancies). Adding this FFT memory to the memory for the storage of the symbol results in 2*N* in normal and $\frac{5}{4}N+1$ in optimized memory word requirement. Unlike the pre-calculated multi-sine signal, the OFDM maintains the flexibility to modify the spectrum of the stimulation signal without the need to reprogram the system.

TABLE I.
MEMORY USED FOR TRADITIONAL EIS APPROACHES AND THE OFDM.

Approach	frequency sweep	Multi-sine worst case	Multi-sine Pre-calculated	OFDM	OFDM Optimized
Memory words (2 bytes)	$\sum_{i=1}^{N/2} \frac{N}{i}$	$\frac{N^2}{2}$	N	$2N$	$\frac{5}{4}N+1$

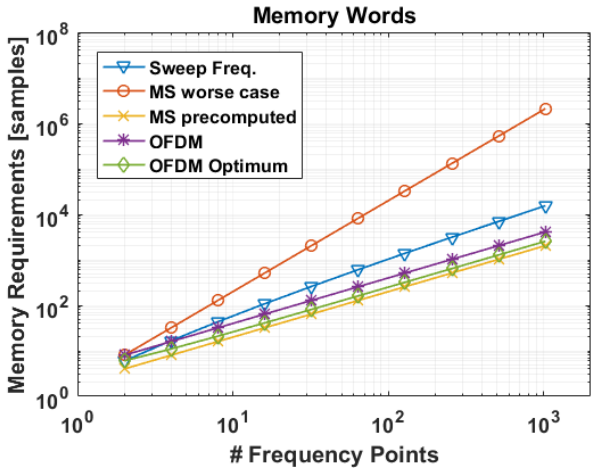

Figure 1. Memory requirements for the generation of the stimulation signal using the frequency sweep, the multi-sine (MS) and the OFDM methods.

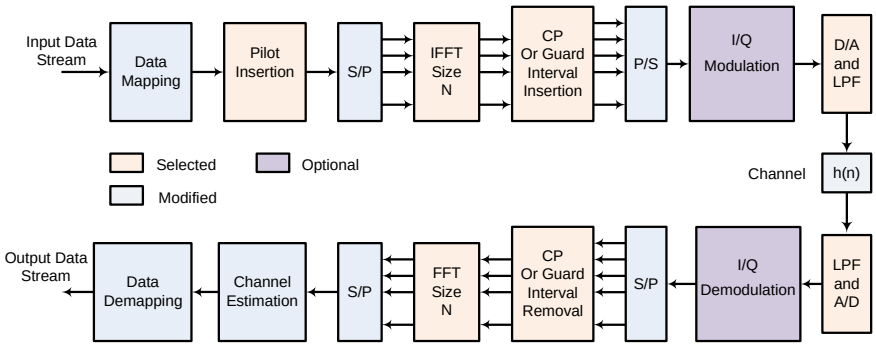

Figure 2. OFDM system blocks showing the selected, modified or optional blocks for the OFDM-EIS system.

3. The OFDM technique for EIS measuring

OFDM is a form of signal modulation that divides a modulating input stream into many modulated narrowband equally-spaced subcarriers. This transformation creates an output signal that contains a flat frequency spectrum within a limited and controllable bandwidth [26]. Therefore, the output of an OFDM transmitter system could be used as a stimulation signal for a fast EIS measurement. The spectrum of such signal can be manipulated by controlling system parameters such as the sampling frequency or the amplitude and size of the input data stream. A typical OFDM system is shown in Figure 2. Here the core of the system are the IFFT/FFT blocks that make the implementation suitable for digital systems.

The OFDM model is adapted for EIS measuring by selecting and modifying some of the blocks as follows:

1. "Data Mapping" and "Data Demapping" blocks are not used in the proposed OFDM-EIS system. Instead, a block that creates OFDM symbols is used. These symbols consist of complex values of constant magnitude, but with phases in quadratic relationship, as shown in equation (1).

$$X(k)=\begin{cases} G & ,k=1 \\ G\cdot e^{\frac{-j2\pi(k-1)^2}{N}} & ,2\le k\le N/2 \\ 0 & ,N/2<k\le N \end{cases} \quad (1)$$

where *X(k)* represents the OFDM symbol, *G* is a constant that controls the output signal amplitude, *k*=1,2,...,*N* and *N* is the IFFT sizes.

The symbol phases produce, at the output of the IFFT, a signal with a reduced crest factor to avoid peaks with high amplitudes that could saturate the DAC, the analog amplifiers or overstimulate biological tissues, such as myocardial cells, and therefore ensure that heart palpitations are not induced during the impedance measurement.

2. Perfect synchronization is required in the OFDM system. Therefore, a Pilot signal is added. This will be explained later in the article.
3. The Serial-to-Parallel (S/P) and Parallel-to-Serial (P/S) conversions are not required in sequential programmable systems.
4. EIS measuring does not suffer from Multipath propagation, whose effects are often eliminated by using the cyclic prefix (CP). Instead, a short guard interval (GI) with zeros will be used to reduce the hardware complexity.
5. The I/Q modulation and demodulation are valid and optional blocks for EIS measuring. However, We consider testing the OFDM technique using a baseband signal, so these blocks have not been implemented in our design. Therefore, even though the output of the IFFT is a sequence of complex values as a function of time, only the real part of them is used, which can be expressed in a polar representation as follows:

$$\mathrm{Re}\{x(n)\}=\frac{G}{N}\left[1+\sum_{k=2}^{N/2}\cos\left(\frac{2\pi(k-1)(n-k)}{N}\right)\right] \quad (2)$$

or, more conveniently, in the rectangular form:

$$\mathrm{Re}\{x(n)\}=\frac{1}{N}\sum_{k=1}^{N/2}\left[a(k)\cdot\cos\left(\frac{2\pi(k-1)(n-1)}{N}\right)+b(k)\cdot\sin\left(\frac{2\pi(k-1)(n-1)}{N}\right)\right] \quad (3)$$

where, $X(k)=a(k)+jb(k)$, $j=\sqrt{-1}$ and n=1,2,...,N.

6. The "Channel Estimation" is modified and called "Impedance Estimation". The method of impedance estimation is explained in section *3.3*.

The objective to design *X(k)* with a first constant value, followed by (*N*/2)-1 complex values and *N*/2 null values is that this one enables the complete recovery of the real and imaginary values of the symbol, *a(k)* and *b(k)*, at the reception of the OFDM system. This is shown in the equation (6). Here, only half of the FFT output is required to recover the N/2 complex OFDM symbols.

At the reception the FFT of size N is performed as shown in equation (4).

$$Y(q)=\sum_{n=1}^{N}\mathrm{Re}\{x(n)\}\cdot e^{\frac{-j2\pi(q-1)(n-1)}{N}} \quad (4)$$

Where replacing equation (3) in (4), result in

$$Y(q)=\frac{1}{N}\sum_{n=1}^{N}\sum_{k=1}^{N/2}\left[a(k)\cdot\cos\left(\frac{2\pi(k-1)(n-1)}{N}\right)\cdot e^{\frac{-j2\pi(q-1)(n-1)}{N}}+b(k)\cdot\sin\left(\frac{2\pi(k-1)(n-1)}{N}\right)\cdot e^{\frac{-j2\pi(q-1)(n-1)}{N}}\right] \quad (5)$$

and finally equation (6) represents the output of the FFT at the receiver side, with q in [1,2, …, N].

$$Y(q)=\begin{cases}a(1)=G & ,q=1\\ \frac{1}{2}\left(a(q)+jb(q)\right) & ,2\le q\le N/2\\ irrelevant & ,N/2<q\le N\end{cases} \quad (6)$$

4. Method

4.1. The OFDM-EIS low cost solution

The OFDM-EIS method is suitable for embedded systems since it can be fully implemented in digital form with high efficiency through the FFT algorithm. During this research work, this technique has been tested experimentally by using a prototype designed for EIS measurement. This implementation uses the capabilities of a "Simblee" module for a compact, wireless, and low power consumption OFDM-based measuring system.

The Simblee RFD77101 module is a high performance Bluetooth radio transceiver with a built-in ARM Cortex M0 microcontroller that can be programmed using the Arduino IDE. The clock frequency is 16 MHz and it includes a 128 kB user application Flash and a 24 kB RAM.

The OFDM-EIS system is based on the Simblee module programmed with a symbol generation block implementing equation (1), a custom 16-bits IFFT/FFT block configurable up to a size of 256, an averaging block, an impedance calculation block and a number of communication routines, as shown in Figure 2. The maximum possible sampling frequency is about 12.05 kHz limited by the 16 MHz Simblee clock frequency and the Bluetooth communication speed [27]. The impedance calculation block performs complex floating point division of the $N/2$ complex calibration samples with the $N/2$ SUT samples after averaging.

As an interface for the analog world a 12-bit digital to analog converter (DAC, MCP4822), a 12-bits analog to digital converter (ADC, MPC3202) and an Analog Front End (AFE) are used. The AFE adapts the signal for the EIS measurements on biological samples, for instance it has an output voltage with a configurable amplitude achieving values in a range from tens to hundreds of millivolts, a low output impedance, near-zero offset of the stimulation signal and an adjustable gain. The electronic board is shown in Figure 5 and measures 6 cm x 7 cm.

4.2. OFDM-EIS function description

As depicted in Figure 2, at every measurement, the mentioned symbol is introduced into the IFFT to create a sequence of N samples that is converted in a voltage signal $x(t)$ by the DAC and then applied to the SUT. Subsequently, the current signal is recovered and digitized by the ADC. The recovered data is converted back to frequency domain by the FFT.

The output of the FFT is a complex value of $2N$ samples: N real samples and N imaginary samples. However, as shown in equation (6), only half of the sample are needed. The

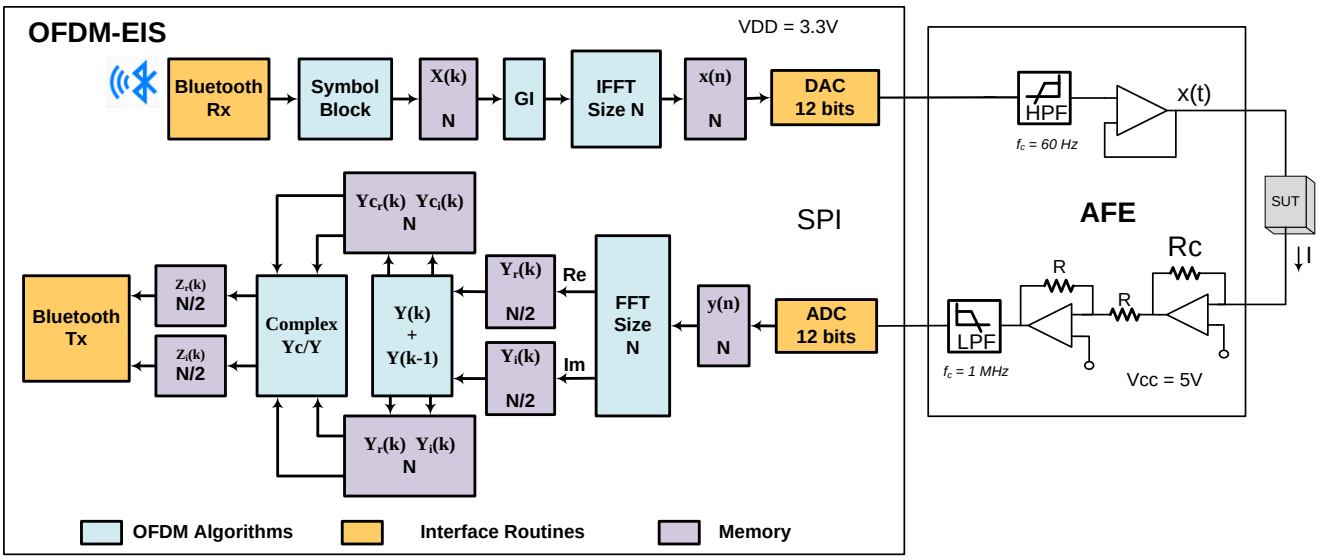

Figure 2. OFDM-EIS System Scheme.

averaging algorithm performs the summation of the previous $N/2$ real and $N/2$ imaginary values with the current ones from the output of the FFT. Next, the impedance calculation block, whose algorithm is detailed the Section 3.3, is fed with the measurement data and the calibration data resulting in the final impedance values.

The impedance value is sent via Bluetooth to a personal computer (PC). The PC runs a software interface, coded in Matlab, for the control of the system and the storage and visualization of the data received wirelessly. The process from the symbol generation up to the FFT computation could be repeated many times in order to reduce noise by averaging.

The custom IFFT/FFT routines are coded for speed improvement and for memory utilization economy. They allow the in-place computation of a complex signed 16-bits data and storing the results in the same input memory space.

4.3. Impedance and crest factor calculation

Since the received signal is an electric current signal, by using the comparison between the calibrated current signal and the SUT current signal the impedance could be calculated, as follows,

$$Z(\omega) = R_C \frac{Y_C}{Y_{SUT}} \tag{7}$$

Where Y_C is the $N/2$ complex calibration data, Y_{SUT} the $N/2$ complex SUT data, R_C is the calibration resistance and Z is the calculated impedance which is a function of the frequency $\omega = 2\pi f$, being f the frequency subcarrier of the OFDM-EIS system.

For the calculation of the crest factor (CF) the following equation is used,

$$CF = \frac{\max(x(t)) - \min(x(t))}{2 \cdot x(t)_{RMS}} \tag{8}$$

Where $x(t)$ is the stimulation signal and $x(t)_{RMS}$ is the root mean squared values of $x(t)$ as shown in equation (9).

$$x(t)_{RMS} = \sqrt{\frac{1}{t_2 - t_1} \int_{t_1}^{t_2} |x(t)|^2 \, dt} \ , \tag{9}$$

being T_1 and T_2 the initial and final time instants when measuring of $x(t)$, respectively.

4.4. Calibration and system synchronization

A critical step during the calibration stage is the measurement of the system delay. This information is used for the correct synchronization of the system. This synchronization is essential to ensure that the selected data block of the FFT corresponds to the IFFT transmitted symbol block.

The method for calibration is the following: before calibration, a pilot signal is used which generates voltage peaks at known intervals. The generated peak can be detected using an appropriate threshold. This method allows the recording of, on one hand, the delay of the transmitter output signal, and on the other, the joint delay of the analog-digital conversion blocks, the AFE and the receiver.

The selection of pilot amplitude is limited by the maximum value allowed for the measurements of biological samples which in our case is limited to 200 mV_{peak}.

5. Experimental setup and results

The proposed OFDM-EIS technique is evaluated by means of the system performance, the quality of the stimulation signal and through experimentation with pacemaker electrodes. For these analyses, the OFDM-EIS system was configured with an IFFT/FFT size N of 64, a sampling frequency F_S of 12.05 kHz and a symbols quantity of 64 with a constant gain G = 200. The other specific aspects of the setup are detailed on their respective section.

5.1. OFDM-EIS system performance

The performance is evaluated through measurement of a electric test circuit with a resistive-capacitive impedance response like the one found on real electrodes [28].

Figure 3 shows the impedance of a test circuit (Rs+Rp||Cp, Rs = 680 Ω, Rp = 4.7 kΩ, Cp = 100 nF) measured by the OFDM-EIS system. Because N = 64 and F_S = 12.05 kHz, there are 32 measured impedance points at the frequencies of $n \cdot F_S/N$, where n=0,1,...,(N/2)-1, and F_S/N = 188.3 Hz is the minimum frequency and also the frequency separation of the points.

The highest measure is at the frequency of 5826.7 Hz. By comparing the measured impedance with the test circuit impedance values the average error of 4.36% was calculated.

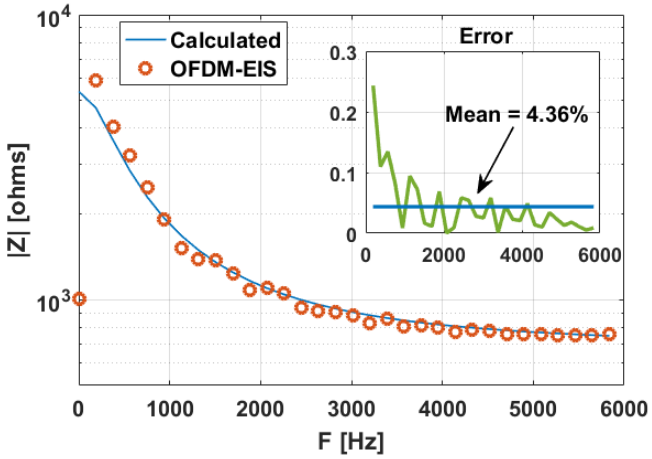

Figure 3. OFDM-EIS impedance measurement of the test circuit. The impedance is compared with the real values of the test circuit. The error plot is depicted inside.

5.2. Power consumption analysis

The system consumption is analyzed through the study of the electric current behavior as a function of time of the OFDM-EIS system, as shown in Figure 4.

The system was tested in the following conditions: it is powered by a 5 V source, regulated to 3.3 V to feed the

Simblee device, there are 64 tones from 188 Hz to 5837 Hz, ten cycles of measurement separated by an idle of 100 ms between cycles, an 560 ohms SUT resistor and the stimulation voltage is 200 mV_{PEAK}.

During the test, the system performed transmission, reception and impedance estimation on every of the ten cycles. It can be noticed that the static consumption of the OFDM board is 15.5 mA. Additionally, the dynamic consumption, when measuring, is about 4 mA that multiplied by the period of one complete OFDM measurement time of 506.6 ms results in a dynamic electric charge of 2.03 mAs or 10.13 mJ, given that the system is powered by a 5 V supply.

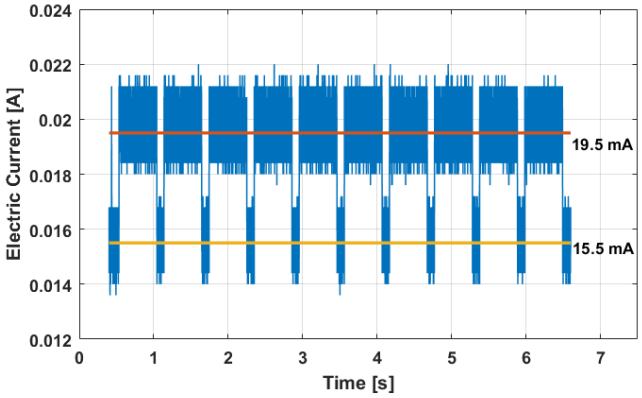

Figure 4. Electric current consumption of the OFDM-EIS system during 10 complete measurements separated by an idle of 100ms.

5.3. Crest factor and sensing time

The crest factor is calculated by measuring the OFDM-EIS output voltage signal with a digital oscilloscope (Tektronic DPO500B).

Figure 5 shows that the amplitude of the signal is below the 200 mV_{PEAK} with a very low offset and with a CF of 1.692 that is very close to the CF calculated by simulation of 1.642. In the simulation the same symbols of integer values, as in the OFDM-EIS system, were used, but with an IFFT of larger bits in their numerical representation. The CF calculation method is shown in Section *4.3.*

The stimulation time is an important factor in our application. It should be less than the time between heart beats. It could be calculated from equation (10). As it is shown in Figure 5, the time of one symbol, when using the OFDM-EIS system with a IFFT size of 64 and a F_S of 12 kHz, is 5.33 ms that gives enough margin for the use of many symbols with the consequent reduction of noise by averaging.

$$S_t = \frac{M \cdot N}{F_S} \tag{10}$$

Where M is the symbols quantity, N is the IFFT size and F_S the sampling frequency.

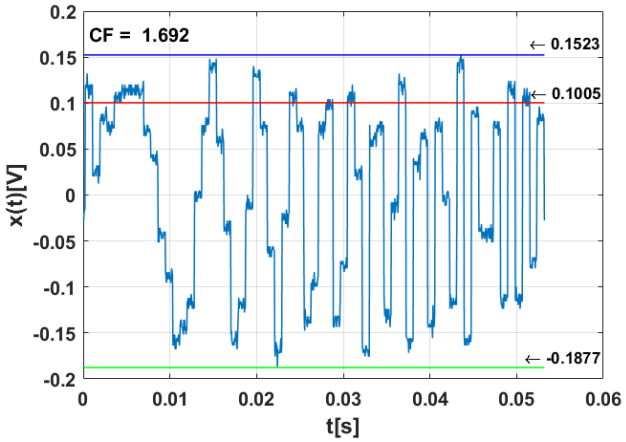

Figure 5. Signal output from the OFDM-EIS system when using the code of equation (1). The CF is calculated and shown as well.

The study of the processing time for the complete OFDM measurement execution has also been performed. This includes the IFFT / FFT computation, the averaging and the impedance calculation. At the reception, the average of the symbols is performed on the fly and only one complex division at the end, hence the time for the calculation of the impedance estimation is not much higher than the stimulation time itself. This time depends on the numbers of instruction required for the averaging and the complex division algorithms as well as the clock frequency of the device.

In our case there are $M{\cdot}N/2$ additions for averaging ($N/2$ real and $N/2$ imaginary) and $N/2$ complex division for the final impedance estimation executed with a clock frequency of 16 MHz. Additionally, the IFFT/FFT algorithm takes about $(N/2)\log_2(N)$ multiplications and the digital to analog to digital conversion blocks, running at 12 kHz, transmit and receive a totality of $N{\cdot}M$ samples. Giving that the clock cycles for each floating point operation for the Cortex M0 processor can be

TABLE 2.
EXECUTION TIME FOR ONE OFDM-EIS MEASUREMENT WHEN $N = M = 64$

Basic Operations:	# of 16 MHz Clock cycles	Time [µs]
Addition	102	6.375
Multiplication	166	10.375
Division	475	29.687

Advance Operations:	Calculation	# of Operations	Time [ms]
Averaging	Additions	$M{\cdot}N/2$	13.056
DAC / ADC	1/12K sample rate	$M{\cdot}N$	341.33
IFFT	$(N/2)LOG_2(N)$	1	1.99
FFT	$(N/2)LOG_2(N)$	M	127.48
Complex Division	3 Additions + 6 Multiplications + 1 Division	$N/2$	3.55
		Total	487.406

known from [30], the total theoretical execution time required to perform one complete OFDM measurement, while using 64 symbols, is calculated as 487.4 ms, as shown in table 2. The real execution time measured from Figure 4, is 506.6 ms which a bit higher than the theoretical one. This result is reasonable considering the time the processor takes for the loops and decision routines.

5.4. Pacemaker's electrode characterization

The potential of the OFDM-EIS system for the impedance characterization of a commercial available human cardiac pacemaker lead (Medtronic CAPSURE VDD-2, bipolar ventricular sensing and pacing lead), shown in Figure 6, is also analyzed. The electrodes of the lead (the tip and the ring electrodes) were both placed into a Phosphate-Buffered Saline (PBS) solution and first characterized by using a commercial Network Analyzer (ENA, Agilent E5061B), configured for impedance measurements, followed by the OFDM-EIS system.

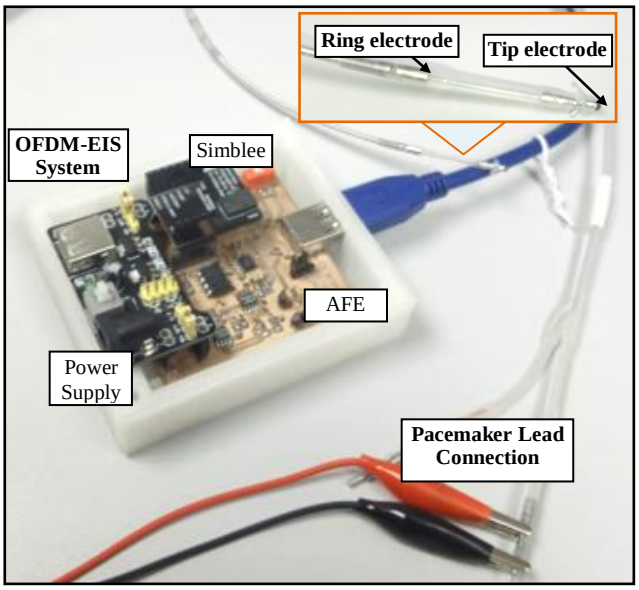

Figure 6. OFDM-EIS system connected to the ventricular sensing and pacing electrode of the pacemaker lead.

Figure 7 shows the electrode's impedances measured by the two systems. It also shows the impedance of an electrode model by taking the OFDM-EIS impedance values as input of a fitting algorithm. The model is the following:

$$Z_{Model} = R_S + \frac{R_P}{1+(j\omega)^{\alpha} C_P R_P} \tag{11}$$

where R_S [Ω] is a serial resistance, R_P [Ω] is a parallel resistance with a no-ideal capacitance C_P [F] that take the place of a constant phase element that is widely employed in the characterization of the electrodes-medium interface [29], and α is dimensionless constant ranging from 0 to 1.

TABLE 3: Model parameters and goodness of fit values

R_S [Ω]	R_P [Ω]	C_P [μF]	α	R-square	RMSE
664	284.8	48.42	0.6106	0.975	8.55

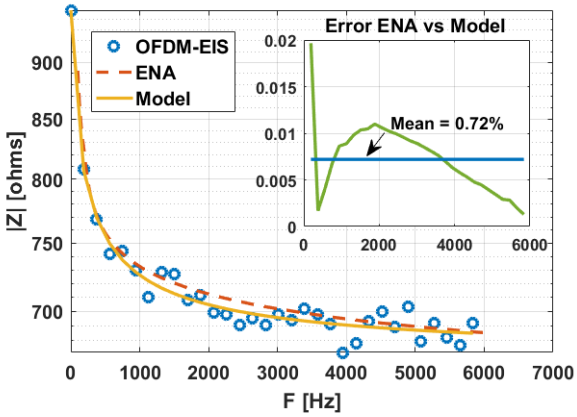

Figure 7. Impedance of a human pacemaker lead in a PBS solution measured with the OFDM-EIS system and the ENA as reference instrument. The impedance of the fitting model and the error when comparing it with the ENA are plotted as well.

The fitting model parameters and the goodness of the fit values are shown in Table 3. The error plot between the ENA and the model impedance values is also depicted in Figure 7. Here an average of 0.72% was calculated.

6. Conclusion and future work

The proposed OFDM-EIS measuring technique allows rapid impedance spectrum estimation with good accuracy. The OFDM symbols are designed with squared phases and with the size of $N/2$ samples that assure a low crest factor and the proper recovery of the real and imaginary part of the symbols from only the real part of the IFFT output data. An ARM-based, custom device implementing the OFDM-EIS method was presented as a low cost solution (less than 50$) for pacemaker-induced fibrosis detection. It was tested with the OFDM parameters of N = 64, F_S = 12.05 kHz, 64 symbols and a symbol gain G = 200. The results show that a crest factor of 1.694 is achieved with the length of 5.33ms per symbol. This time is short enough to even use many symbols for the reduction of noise and still accomplish the requirement time for the measurement of pacemaker-induced fibrosis impedance. Furthermore, an average error of 4.4% is obtained when measuring a test circuit and an average error of 0.72% is achieved when characterizing a human pacemaker lead electrodes by using the OFDM-EIS results as input of a fitting model. The measurement spectrum could easily be manipulated from the OFDM system parameters by controlling the sampling frequency and/or the size of the IFFT, providing a good flexibility to the method. To further improve the accuracy of the measurement without much affecting the CF, the constant gain G could be changed into a variable, as a function of k, that can be adjusted with the help of a searching

algorithm. Also, a small offset could be added to the symbols to increase further the subcarriers amplitudes and therefore the accuracy. These topics are part of a current study in our group.

Acknowledgements

The work by this author was partially supported by the National Secretary of Science and Technologic (SENACYT) of Panamá.

References

[1] N. Lewis et al., Relevance of impedance spectroscopy for the monitoring of implant-induced fibrosis: A preliminary study, IEEE Biomedical Circuits and Systems Conference (BioCAS) , pp. 1-4, 2015.

[2] S. De Jong, T. A. B. Van Veen, J. M. T. De Bakker, M. A. Vos, and H. V. M. Van Rijen, Biomarkers of myocardial fibrosis, J. Cardiovasc. Pharmacol., vol. 57, no. 5, pp. 522–535, 2011.

[3] G. C. McConnell, R J Butera and R V Bellamkonda, Bioimpedance modeling to monitor astrocytic response to chronically implanted electrodes, J. Neural Eng. 6, 2009.

[4] N. Akoum, C. McGann, G. Vergara, T. Badger, R. Ranjan, C. Mahnkopf, E. Kholmovski, R. MacLeod, and N. Marrouche, Atrial fibrosis quantified using Late Gadolinium Enhancement MRI is associated with sinus node dysfunction requiring pacemaker implant, J. Cardiovasc. Electrophysiol., vol. 23, no. 1, pp. 44–50, 2012.

[5] Yokoyama K, Kariyasu T, Kuhara S, Imai M, Ishimura R, et al., Influence of MRI-Conditional Cardiac Pacemakers on Quality and Interpretability of Images Acquired in 1.5-T Cardiac MRI, Int. J. Clin. Cardiol., 2:030, 2015.

[6] P. Héroux and M. Bourdages, Monitoring living tissues by electrical impedance spectroscopy, Ann. Biomed. Eng., vol. 22, no. 3, pp. 328–337, 1994.

[7] M. Grossi and B. Riccò, Electrical impedance spectroscopy (EIS) for biological analysis and food characterization: A review, J. Sensors Sens. Syst., vol. 6, no. 2, pp. 303–325, 2017.

[8] B. Sanchez, X. Fernandez, S. Reig and R. Bragos, An FPGA-based frequency response analyzer for multi-sine and stepped sine measurements on stationary and time-varying impedance, IOP Publishing Ltd, Measurement Science and Technology, November 23, 2013.

[9] Friedrich, J & Helbig, M & Barthel, A & Nacke, Thomas & Sachs, J & Schäfer, M & Peyerl, P & Pliquett, U. A new hard and software concept for impedance spectroscopy analysers for broadband process measurements, 13th International Conference on Electrical Bioimpedance and the 8th Conference on Electrical Impedance Tomography: ICEBI 2007, August 29th - September 2nd 2007, Graz, Austria (pp.194-197).

[10] Engels, M. (2005). Wireless OFDM systems. Dordrecht: Kluwer Academic Publishers.

[11] B. R. Ballal, A. Chadha, and N. Satam, Orthogonal Frequency Division Multiplexing and its Applications, Int. J. Sci. Res., vol. 2, no. 1, pp. 325–328, 2013.

[12] M. Vucha and L. S. Varghese, Design Space Exploration of DSP Techniques for Hardware Software Co-Design : An OFDM Transmitter Case Study, Int. J. Comput. Appl., vol. 116, no. 20, pp. 29–33, 2015.

[13] P. R. K. Paliwal, C. M. Jadhao, and P. A. S. Kakad, Review on FPGA Implementation of OFDM, Int. J. Comput. Sci. Inf. Technol., vol. 5, no. 5, pp. 6116–6120, 2014.

[14] Calculation principles of RTCA Software, Technical Note No. 2, xCELLigence System, Jan. 2010.

[15] S. Gabriel, R. Lau, and C. Gabriel, The dielectric properties of biological tissues : II. Measurements in the frequency range 10 Hz to 20 GHz, Phys. Med. Biol., vol. 41, pp. 2251–2269, 1996.

[16] G. Blanc, I. Epelboin, C. Gabrielli, and M. Keddam, Measurement of the elecrode impedance in a wide frequency range using pseudo-random noise, Electrochim. Acta, vol. 20, no. 8, pp. 599–601, 1975.

[17] M. Cohn and A. Lempel, On Fast M-Sequence Transforms, IEEE Trans. Inf. Theory, vol. 23, no. 1, pp. 135–137, 1977.

[18] I. Schneider, Broadband signals for electrical impedance measurements of long bone fractures, 18th Annu. Int. Conf. IEEE Eng. Med. Biol. Soc., pp. 1934–1935, 1996.

[19] T. Sun, C. van Berkel, N. G. Green, and H. Morgan, Digital signal processing methods for impedance microfluidic cytometry, Microfluid. Nanofluidics, vol. 6, no. 2, pp. 179–187, 2009.

[20] R. Bragos, R. Blanco-Enrich, O. Casas, and J. Rosell, Characterisation of dynamic biologic systems using multi-sine based impedance spectroscopy, IMTC 2001. Proc. 18th IEEE Instrum. Meas. Technol. Conf. Rediscovering Meas. Age Informatics (Cat. No.01CH 37188), vol. 1, no. 1, pp. 44–47, 2001.

[21] T. Breugelmans, E. Tourwé, J. B. Jorcin, A. Alvarez-Pampliega, B. Geboes, H. Terryn, and A. Hubin, Odd random phase multi-sine EIS for organic coating analysis, Prog. Org. Coatings, vol. 69, no. 2, pp. 215–218, 2010.

[22] B. Sanchez, G. Vandersteen, I. Martin, D. Castillo, A. Torrego, P. J. Riu, J. Schoukens, and R. Bragos, In vivo electrical bioimpedance characterization of human lung tissue during the bronchoscopy procedure. A feasibility study, Med. Eng. Phys., vol. 35, no. 7, pp. 949–957, 2013.

[23] B. Sanchez and R. Bragos, Fast Electrical Impedance Spectroscopy for Moving Tissue Characterization Using Bilateral QuasiLogarithmic Multi-sine Bursts Signals, IFMBE Proc., vol. 22, pp. 1084–1087, 2008.

[24] E. De Roux, M. Terosiet, F. Kolbl, M. Boissière, E; Pauthe, et al., Toward an Embedded OFDM-based System for Living Cells Study by Electrochemical Impedance Spectroscopy, Proceedings of IEEE HealthCom Conference, Sep 2018, Ostrava, Czech Republic.

[25] S. B. Weinstein and M. Ebert, Paul. Data Transmission by Frequency-Division Multiplexing Using the Discrete Fourier Transform, Communication Technology, IEEE Transactions no. 19, 628 - 634, 1971, doi: 10.1109/TCOM.1971.1090705.

[26] H. Shulze and C. Lüders, Theory and Applications of OFDM and CDMA, John Wiley & Sons, 2005.

[27] RF Digital Corporation, "RFD77101 DATASHEET v1.0", 2015, www.simblee.com.

[28] P. Héroux and M. Bourdages, Monitoring living tissues by electrical impedance spectroscopy, Ann. Biomed. Eng., vol. 22, no. 3, pp. 328–337, 1994.

[29] E. Barsoukov and J. R. Macdonald, Impedance Spectroscopy: Theory, Experiment, and Applications, Wiley online library, doi:10.1002/0471716243, 2005.

[30] Quinapalus, https://www.quinapalus.com/qfplib.html. Visited on April 2019.